Journal of Environment and Earth Science
ISSN 2224-3216 (Paper) ISSN 2225-0948 (Online)
Vol.6, No.7, 2016 www.iiste.org

Palaeocurrent and Petrographic Evaluations of Sandstones in the Cretaceous Gulani Formation of the Eastern Gongola Basin, North-east Nigeria: Its Implication for Provenance Studies

J. Ayok
Department of Geology, Federal University Lokoja, Lokoja, Nigeria

Abstract
The Turonian Gulani Formation of north-eastern Nigeria is characterized by a dominant subfacies represented by tabular cross-bedded, medium to very coarse-grained quartz arenites and granulestones with individual sets frequently several metres thick. The palaeocurrent indicates an easterly source area with the main focus of sediment influx located around latitude 10°46' north, the point of origin, on a gross scale, of a deltaic body. Within this body, small Gilbert-type delta lobes are thought to have formed in association with the major delta distributary channels. Petrographically the cross-bedded sandstone subfacies is medium to very coarse-grained, poorly to well sorted, sub-angular to well rounded quartz arenite, consisting of majorly monocrystalline quartz and rare polycrystalline quartz with a kaolinitic matrix. This subfacies is characterized by the extreme rarity or absence of feldspar, low diversity heavy mineral suites and the presence of sedimentary rock fragments, suggesting a sedimentary source area, probably in large part comprising Late Cenomanian to Early Turonian littoral sands deposited during a major preceding transgression.
Keywords: Turonian; Gulani Formation; north-east Nigeria, tabular cross-bedded sandstone subfacies; paleocurrent directions; Late Cenomanian to Early Turonian reworked littoral sands.

INTRODUCTION

The term provenance is derived from the Latin verb "provenire", meaning to come forth or to originate. In its broadest scope, provenance analysis includes all investigation that would aid in reconstructing the lithospheric history of the Earth (Basu, 2003).

In sedimentary petrology, the term provenance has been used to encompass all factors related to the generation of sediment, with specific reference to the composition of the parent rocks as well as the physiography and climate of the source area from which sediment is derived (Weltje and von Eynatten, 2004).

Therefore, the ultimate goal of provenance studies is to deduce the characteristics of source areas from measurements of compositional and textural properties of sediments, supplemented by information from other lines of evidence (Pettijohn et al., 1987).

Suitable analytical approaches to sediment provenance therefore also depend on grain size (Weltje and von Eynatten, 2004). According to them, successful methods to analyse, sand-sized sediments may not be applicable to finer grained materials. Cobbles and boulders potentially allow application of the full range of analytical methods that are used to study the primary source rocks, because the original mineral paragenesis is preserved and can be used to estimate metamorphic pressure–temperature–time paths (Cuthbert 1991). But in the case of finer grained sediments, they often lost all paragenetic information due to decomposition into individual mineral grains, as well as chemical and/or mineralogical transformations (Weltje and von Eynatten, 2004).

The Benue Trough is an elongated northeast to southwest trending mega- structure, extending from Niger Delta in the south as far as the Chad Basin in the north and forming part of the West African Rift System of Fairhead (1986) and subsequent authors. This mega-structure is approximately 1000 km long and 120-150 km wide, and lies within the Pan African mobile belt of West Africa (Guiraud, 1990). It contains up to 6000 m of Cretaceous to Tertiary sediments and associated volcanics. The mechanism responsible for the origin and evolution of the Benue Trough is still a subject of controversy. However, there are essentially two models; the rift and the pull-apart models. Zaborski (2003) reiterated that evidences of both models are clearly manifested within the trough, and therefore concluded the origin of the Benue Trough is best regarded as a rift superimposed on it with sinistral strike-slip faults. The trough is conventionally subdivided into three sectors; the lower Benue Trough, middle Benue Trough and the upper Benue Trough. The upper Benue Trough bifurcates into the N-S trending Gongola arm/ Basin and the E-W trending Yola arm (Fig.1).

The stratigraphic succession in the Gongola Basin has been described by Carter *et al*. (1963), Popoff *et al*. (1986) and Zaborski *et al*. (1998). Most recently, Hamidu *et al*. (2013) and Ayok *et al*. (2014) proposed modifications for the Upper Cretaceous lithostratigraphic successions of the western and eastern Gongola Basin, respectively (Table 1).

For the eastern Gongola Basin, Zaborski *et al.* (1998) recognized a "Kanawa Member" and an upper "Gulani Member" within the Pindiga Formation of previous authors. The former comprised transgressive shales and thin limestones of Late Cenomanian to Early Turonian and the latter sandy regressive deposits of

Journal of Environment and Earth Science www.iiste.org
ISSN 2224-3216 (Paper) ISSN 2225-0948 (Online)
Vol.6, No.7, 2016

probable Middle Turonian age.

Ayok and Zaborski (2014) interpreted the Gulani Formation as mainly comprising small-scale Gilbert-type delta lobes (represented by large-scale tabular cross-bedded sandstones and granulestones) prograding over shallow sublittoral interbedded shales and sandstones, or over each other.

Ayok *et al*. (2014) upgraded both the Kanawa and Gulani members of the "Pindiga Formation" to formational status, while the Pindiga Formation was upgraded to group status (see Table 1), additionally a geological map of the area was produced (see Fig.2). A type section (lectostratotype) was designated for the Gulani Formation (see Fig.3) and additional reference sections (Figs. 4 and 5) too by the same authors.

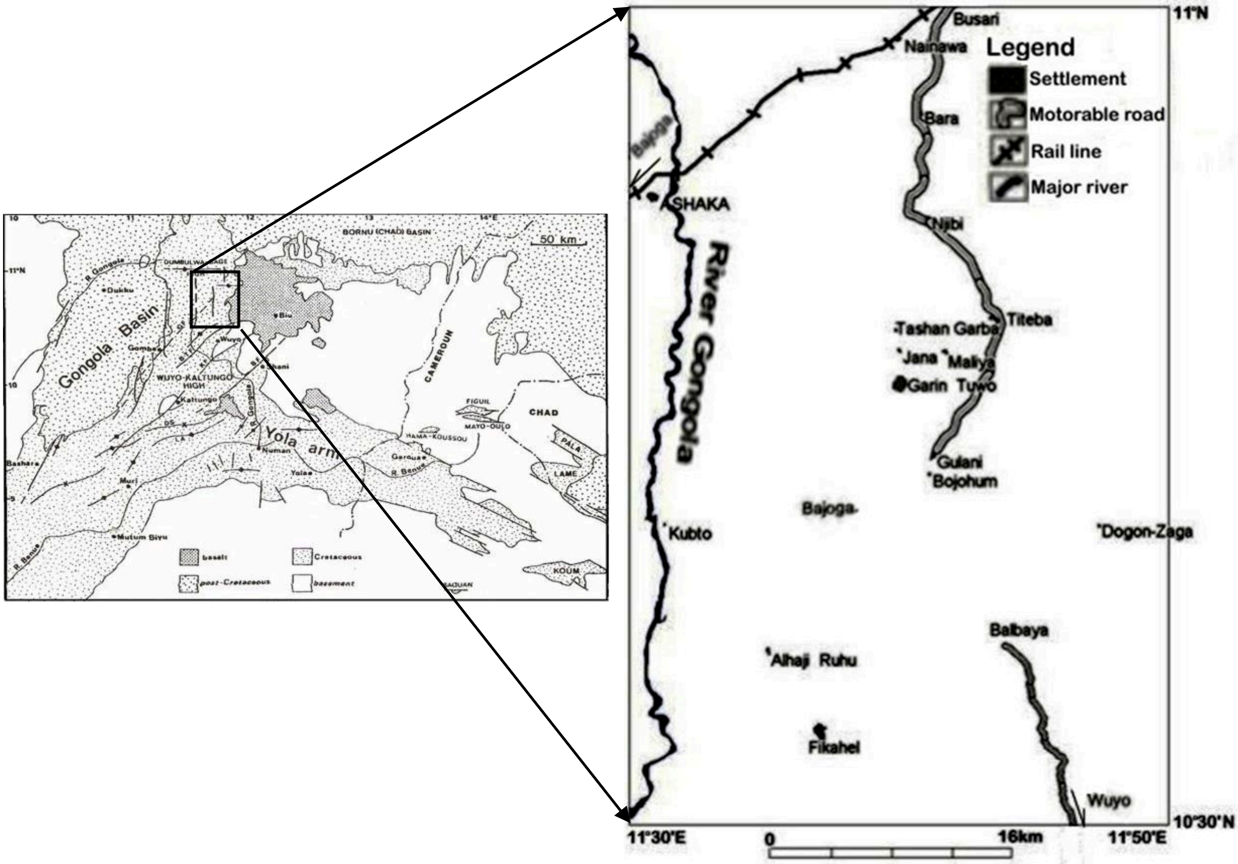

Figure 1. Outline geological map showing the main features of the upper Benue Trough region; GF-Gombe Fault; B-TF-Bima-Teli Fault; KF-Kaltungo Fault; BF-Burashika Fault; DS-Dadiya syncline; LA-Lamurde anticline (After Zaborski 1998). The blocked area represents the study area).

Table 1.Upper Cretaceous and younger lithostratigraphic succession in the western and eastern parts of the Gongola Basin as proposed by Hamidu *et al*. (2013) and Ayok *et al*. (2014). (E-Early, M-Middle, L-Late, D.F-Deba Fulani and D-Dumbulwa).

		W.Gongola Basin (Hamidu et al.,2013)	E.Gongola Basin (Ayok et al.,2014)	Environment of deposition
Quaternary-Neogene			Biu Basalts (& dolerite intrusion)	
Paleocene		Kerri-Kerri Formation		Continental
Maastrichtian		Tukulma Group: Duguri Member; Arowa Member; Upper Fika Member		Continental to marine
Campanian				Compression/ uplift and erosion
Santonian				
Conaician		Lower Fika Member		Marine
Turonian	L			
	M	D.F.Member/D.Member	Pindiga Group: Gulani Formation	Shallow marine
	E	Kanawa Member	Pindiga Group: Kanawa Formation	Marine
Cenomanian		Yolde Formation	Yolde Formation	Transitional
		Upper Bima Formation (upper part)	Upper Bima Formation (upper part)	Continental

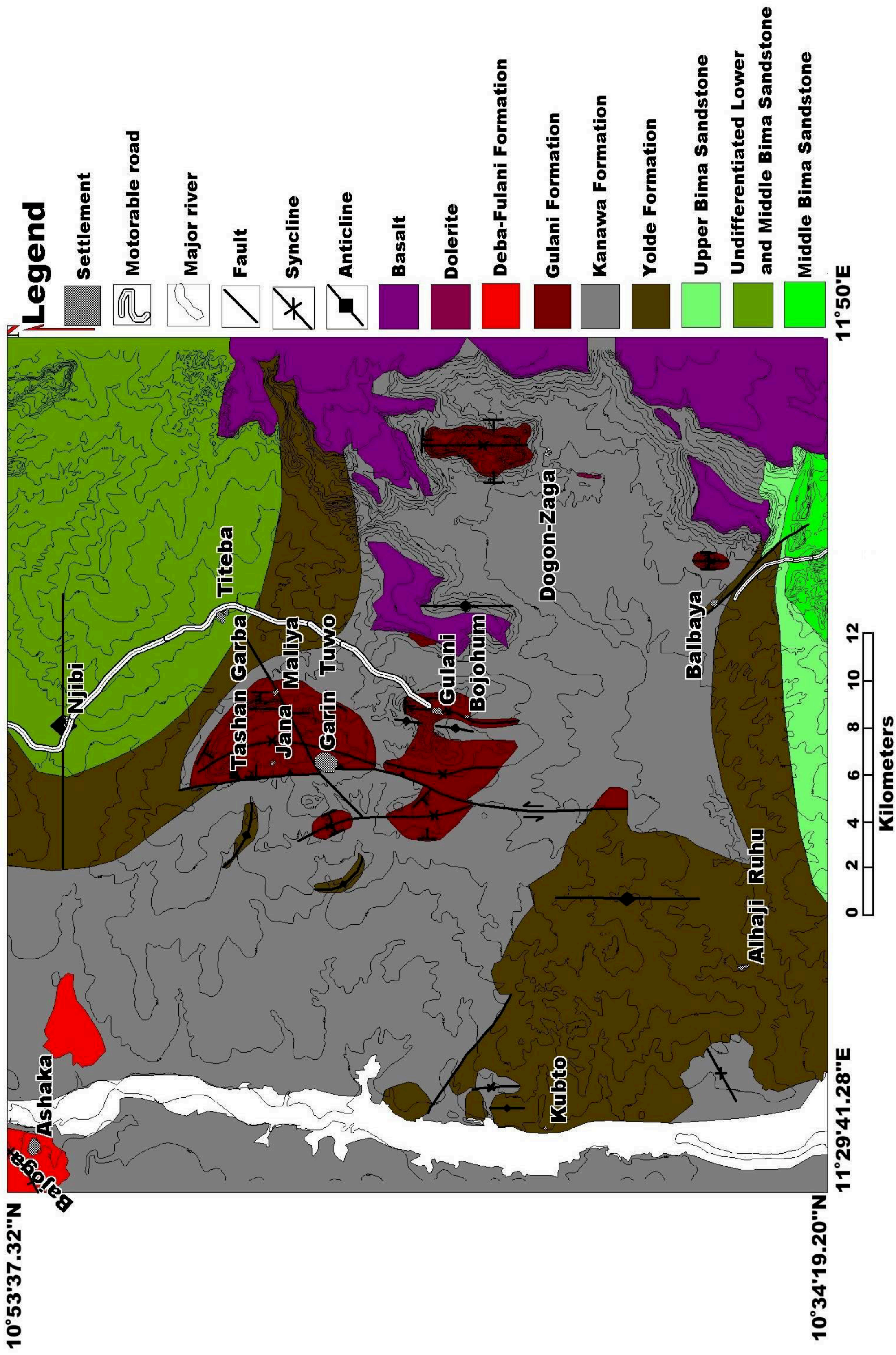

Figure 2.Geological map of the study area after Ayok *et al.* (2014).

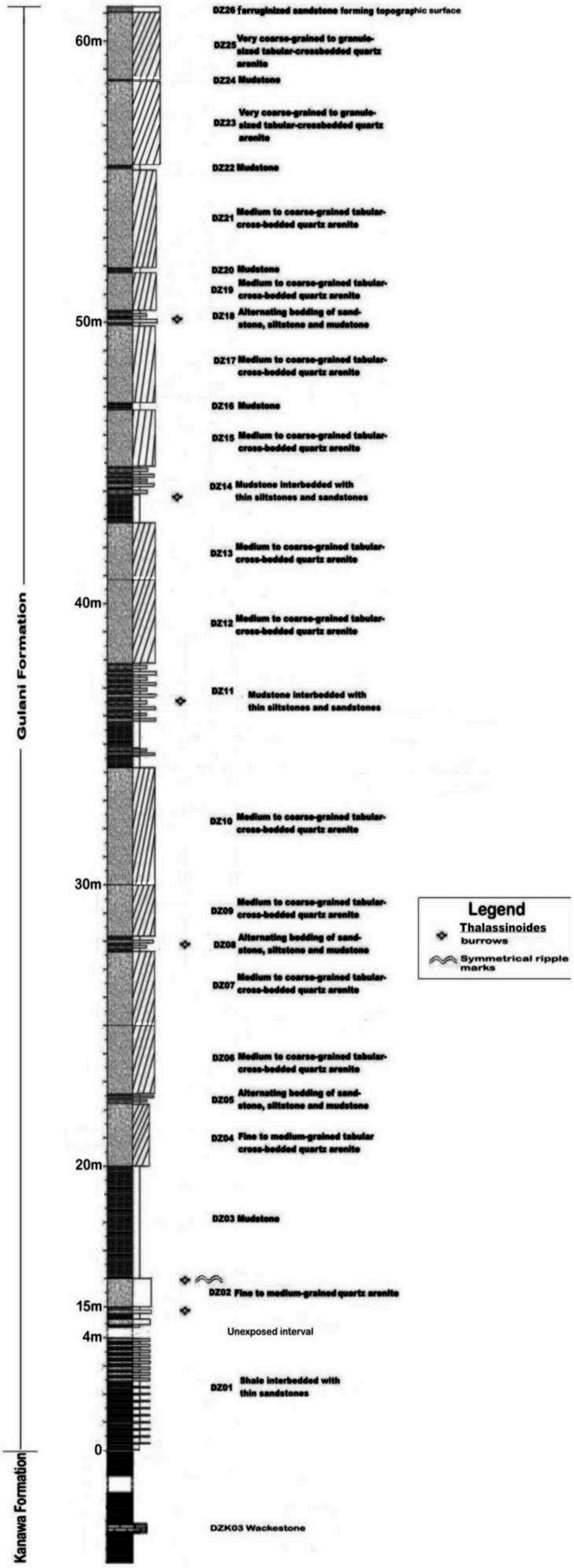

Figure 3. Lithostratigraphic log of the type section of the Gulani Formation exposed north-east of Dogon Zaga; base: 10º41'29.4"N and 11º39'57.9"E; top: 10º41'36.1"N and 11º47'45.8"E (after Ayok *et al*. 2014).

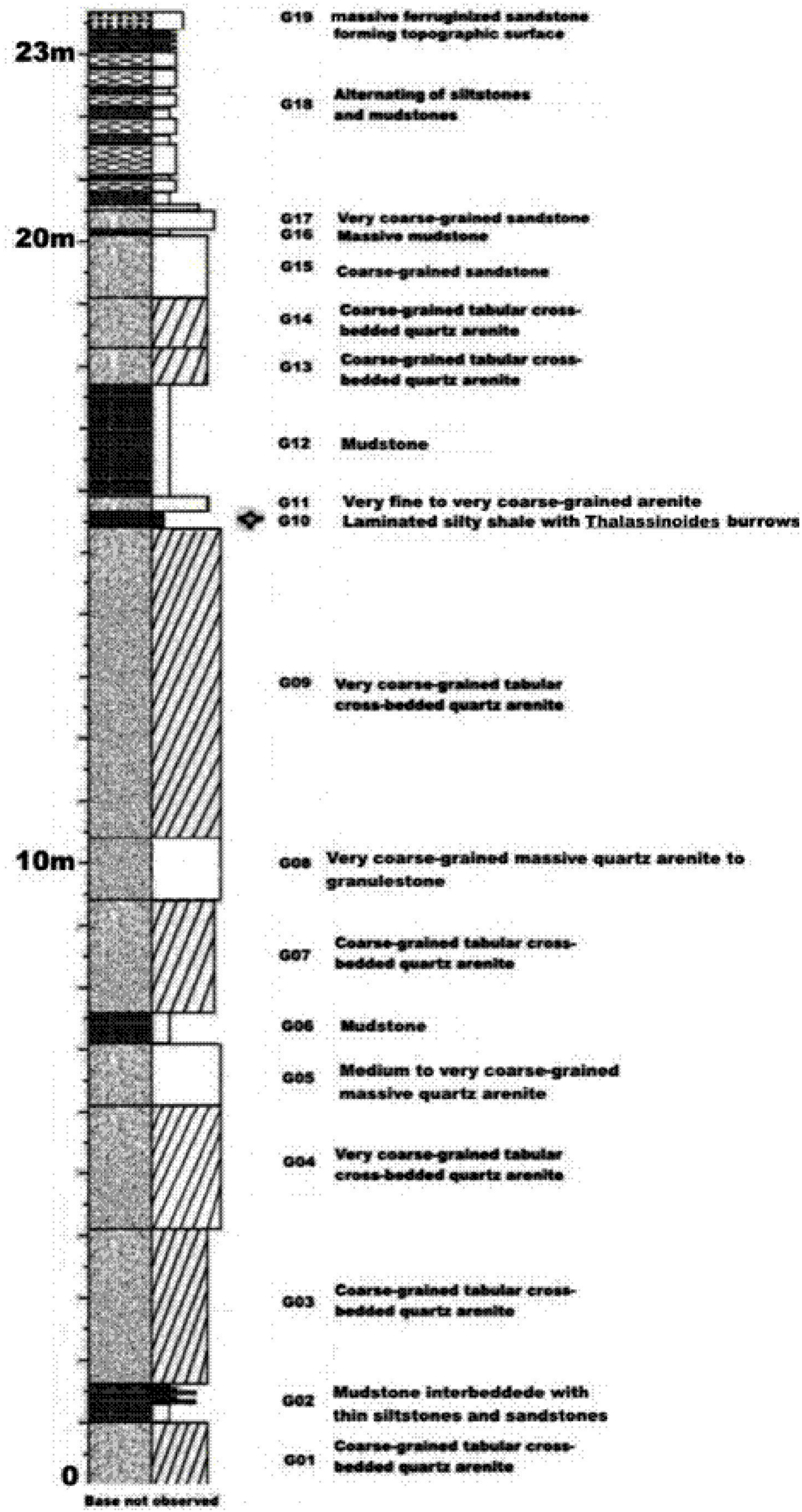

Figure 4. Lithostratigraphic log of the Gulani Formation exposed 750 m north of Gulani; base of section: N10^{o}41'12" and E11^{o}48'06" (After Ayok *et al*. 2014).

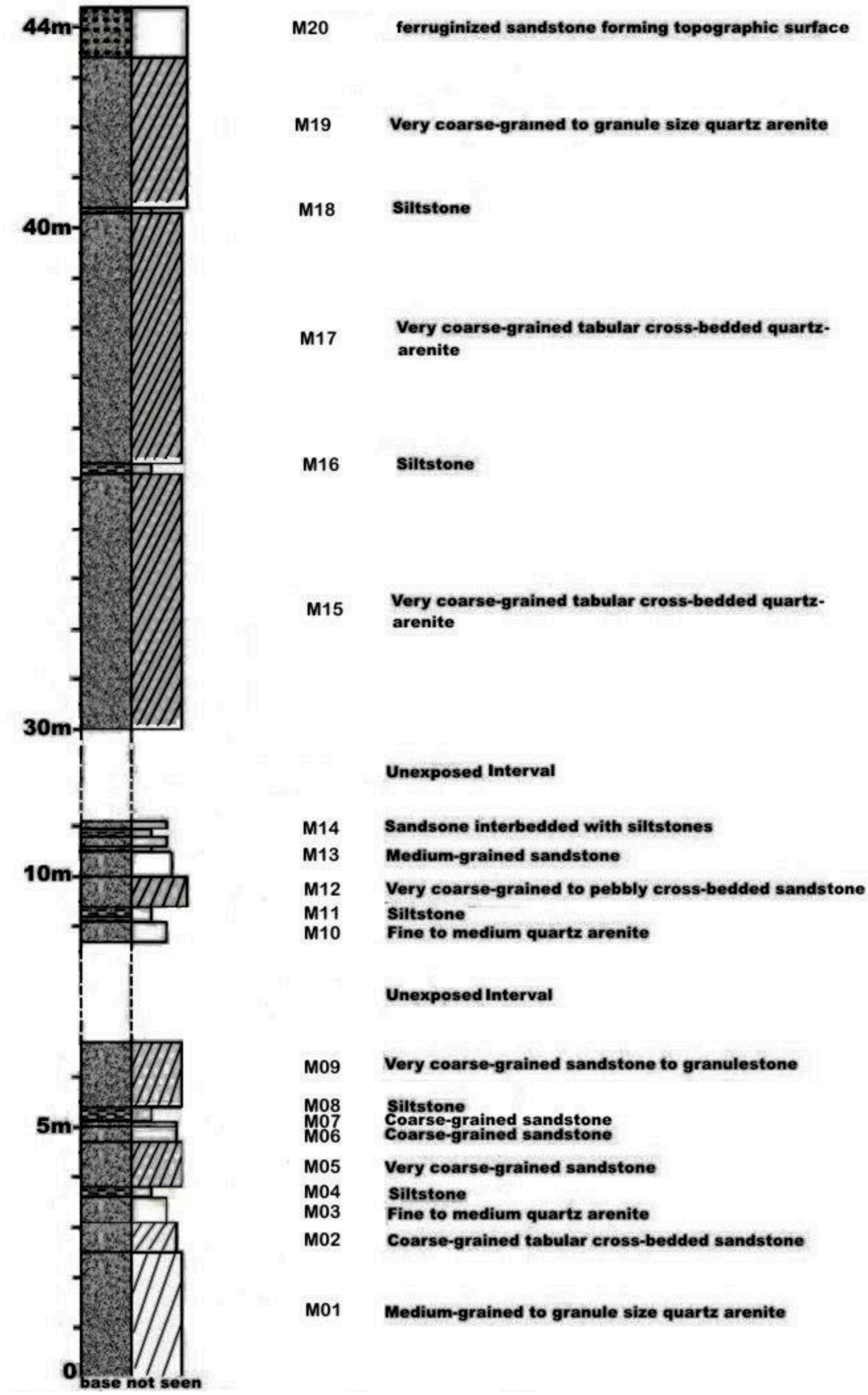

Figure 5. Lithostratigraphic log of the Gulani Formation exposed 100 m west of Maliya;base:N10°47'08" and E11°41' 25"(after Ayok *et al*. 2014).

METHODOLOGY

Field measurement

Measurement of foresets within the cross-bedded sandstone units of the Gulani Formation were obtained in the field with help of compass clinometers, thereafter the direction of inclination of foresets were corrected for tectonic dip using the procedure of Turcker (1996; page 120-121) and the results presented in Appendix VI.

Thin Section and Microscopic Studies

A total of twenty one (21) outcrop samples of sandstones from the "Gulani Formation were selected for thin sectioning. The samples are weakly undurated and were impregnated in a vacuum chamber before they were thin sectioned in the Department of Earth Science, University of Silesia, Poland. Petrographic studies and photomicrography were carried out for all the thin sections with the help of a trinocular petrological microscope in the Department of Geology, Ahmadu Bello University, Zaria.

Heavy Mineral Analysis. A total of twenty one samples from the sandstone dominated facies were subjected to heavy mineral analysis in the sedimentology Laboratory of the Department of Geology, Ahmadu Bello University, Zaria. The sandstones were sieved to obtain the very fine-sand to fine-sand fractions because the satisfied the size fraction common to all samples, the modal class of the coarse fraction and the size fraction likely to contain the highest percentage of heavy minerals. Two grammes of each of the samples was weighed and poured into the centrifuge tubes containing 10 mls of bromoform. The centrifuge tubes were inserted in their respective holes in the centrifuge and the cover closed before running the machine for 10 minutes. This was followed by standard methods for separation of heavy minerals from lighter ones. The heavy minerals were finally identified with the help of binocular microscope.

PALAEOCURRENT ANALYSIS RESULT

Palaeocurrent data obtained from foresets (see appendices A.1 to A.4) within the large-scale cross-bedded sandstones within the Gulani Formation is shown in Figure 6. Corrections were first made for the effects of tectonic dip. As a result of strike-slip faulting some unquantified rotation of the beds about vertical axes has also taken place in the Jana region, but its effects were relatively minor in terms of palaeocurrent direction. The individual sites from where paleocurrent direction data were obtained all show a unimodal pattern (fig.6). The regional pattern suggests a number of delta lobes radiating from a source centred around present-day latitude of 10º46' north (fig.6).

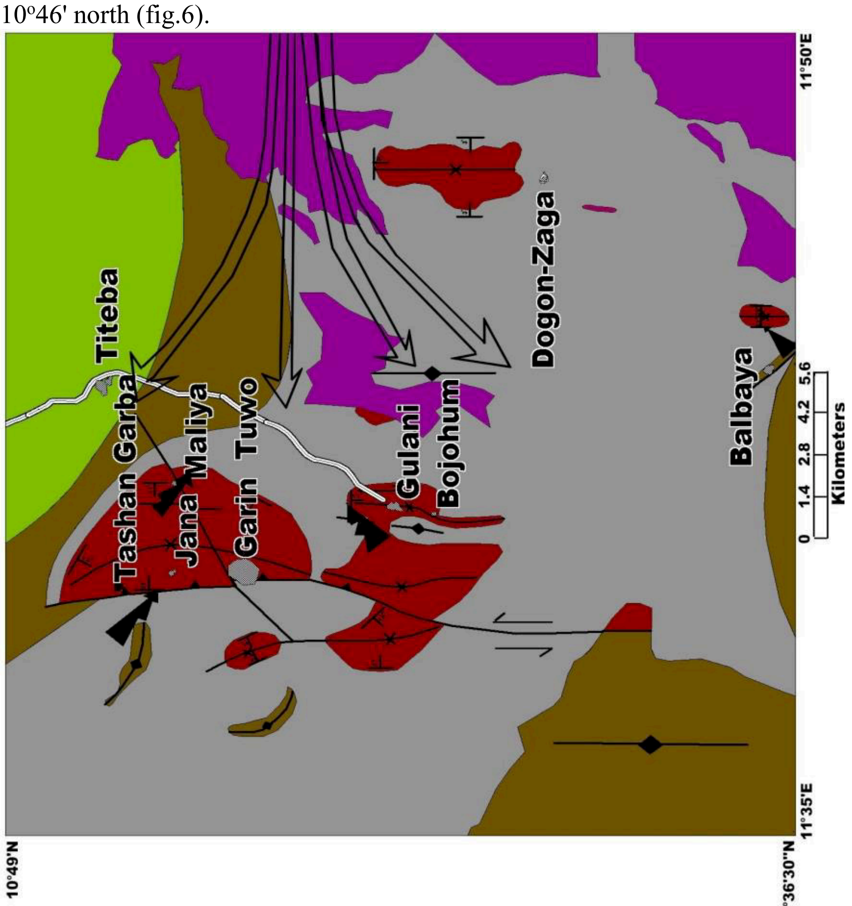

Figure 6.Detailed geological map of the central portion of the study area with palaeocurrent data for the Gulani Formation.

PETROGRAPHIC ANALYSIS RESULT

Results of textural and compositional properties of 20 sandstones samples from the Gulani Formation are shown in table 2, while some selected corresponding photomicrographs shown in appendices B.1 to B.3. From the table, the sandstones from the Gulani Formation are generally medium to very coarse-grained, moderately sorted to well sorted, subangular to rounded quartz arenites and granulestones and rare quartz wackes. Feldspar is frequently totally lacking; sedimentary rock fragments occur infrequently (see Fig.7).

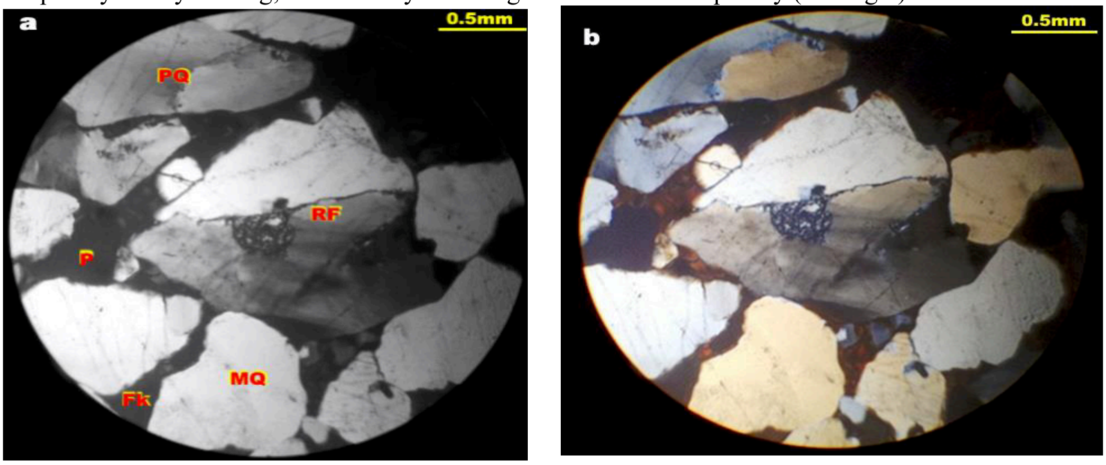

Figure 7. Photomicrograph of Gulani Formation, 750 m west of Jana (WJ02 see figure 2; 10º46'29"N and 11º39'15"E); comprising coarse-grained sand to granule-sized, moderately sorted, sub-rounded quartz arenite consisting of monocrystalline quartz, polycrystalline quartz and a sedimentary rock fragment (comprising quartz grains enclosing authigenic pore-filling kaolinite) and pore-filling ferruginized kaolinite cement. (P-pore space; PQ-polycrystalline quartz; MQ-monocrystalline quartz; RF-rock fragment; Fk-ferruginized kaolinite). a) PPL and b) XPL.

Results from heavy mineral analysis using bromoform indicate that the sandstones from the Gulani Formation have low diversity mineral suite, and are dominated by tourmaline, zircon and opaques.

Table 2. Petrographic results showing textural and compositional properties of sandstones from the Gulani Formation.

Sample No.	Textural properties			Compositional properties (Framework Elements)				Matrix	Cement
	Grain Size	Sorting	Roundness	Monocrystalline Quartz	Polycrystalline Quartz	Feldspar	Rock Fragment		
DZ25	very coarse-grained sand to granule-sized	moderately to well sorted	sub-rounded to well rounded	> 98%	< 2%	Nil	Nil		ferruginized kaolinite
DZ21	medium to very coarse-grained	poorly to moderately sorted	sub-angular to sub-rounded	> 98%	< 2%	Nil;	Nil		ferruginized kaolinite
DZ17	coarse to very coarse-grained	well sorted	sub-angular to subrounded	> 98%	< 2%	Nil	Nil		ferruginized kaolinite, illite rim
DZ12	medium to coarse-grained	moderately sorted	subangular to subrounded	> 98%	< 2%	Nil	Nil		ferruginized kaolinite
DZ10	medium to coarse-grained	moderately well sorted	sub-angular to sub-rounded	> 98%	< 2%	Nil	Nil		ferruginized kaolinite cement
DZ04	fine to medium-grained	moderately to well sorted	sub-angular to sub-rounded	> 98%	< 2%	Nil	Nil		ferruginized kaolinite, quartz overgrowth
DZ02	fine to medium-grained	very well sorted	subangular to subrounded	> 98%	< 2%	Nil	Nil		extensive quartz overgrowth
G13	very coarse-grained	well sorted	sub-angular to sub-rounded	> 98%	< 2%	Nil	Nil		ferruginized kaolinite
G11	very fine to very coarse-grained	poorly sorted	sub-angular to sub-rounded	100%	Nil	Nil	Nil	Silt-grade quartz and clays	Kaolinite, illite rim
G09	coarse-grained	well sorted	angular to sub-rounded	> 95%	< 5%	Nil	Nil		ferruginized kaolinite
G07	medium to coarse-grained	well sorted	sub-angular to sub-rounded	> 95%	< 5%	Nil	Nil		ferruginized kaolinite
G05	medium to very coarse-grained	well sorted	sub-angular to sub-rounded	> 95%	< 5%	Nil	Nil		ferruginized kaolinite, quartz overgrowth
G04	medium to coarse-grained	well sorted	sub-angular to rounded	> 95%	< 5%	Nil	Nil		ferruginized kaolinite
G01	medium to very coarse-grained	moderately sorted	sub-angular to sub-rounded	> 98%	< 2%	Nil	Nil		ferruginized kaolinite
M21	very coarse-grained	well sorted	sub-angular to rounded	> 95%	< 5%	Nil	Nil		ferruginized kaolinite, quartz overgrowths, illite rim
M19	medium to coarse-grained	moderately sorted	sub-angular to sub-rounded	> 98%	< 2%	Nil	Nil		ferruginized kaolinite
M10	fine to medium-grained	well sorted	sub-rounded	> 99%	< 1%	Nil	Nil		ferruginized kaolinite
M01	medium-grained sand to granule size	moderately sorted	sub-angular to sub-rounded	> 95%	< 5%	Nil	Nil		ferruginized kaolinite
WJ01	medium to very coarse-grained	poorly sorted	sub-angular to sub-rounded	> 99%	< 1%	Nil	Nil	Silt-grade quartz, kaolinitic clays	kaolinite
WJ02	coarse-grained sand to granule-sized	moderately sorted	sub-rounded	> 95	> 2%	Nil	< 2% (of sedimentary origin)		ferruginized kaolinite

Note; DZ (Dogon Zaga; Gulani Formation type section; figure 3), G (Gulani Section; figure4), M (Maliya Section; figure 4) and WJ (west of Jana;)

DISCUSSION ON IMPLICATION IN PROVENANCE STUDIES

Since there is no evidence of its diagenetic loss, the extreme rarity or absence of feldspar may be the result of either: its almost complete decomposition in the source rocks; or its loss through reworking of a sedimentary source rock; or both.

A sedimentary source is supported by the low diversity heavy mineral suite and the presence of sedimentary rock fragments.

The deposition of the Kanawa Formation coincided with the major Late Cenomanian to Early Turonian transgression that affected the entire Benue Trough and also Sahara regions to the north (Busson, 1972; Reyment, 1980; Meister *et al.,* 1992). As pointed out by Zaborski (2000, p.157), however, the exact geographical extent of the sea in the upper Benue Trough has been difficult to determine as its marginal marine lithofacies (littoral facies) are rarely observed. During the mid-Turonian regressive conditions set in leading to deposition of Gulani Formation and its lateral equivalents elsewhere in the Gongola Basin, the Deba Fulani and Dumbulwa members (Zaborski *et al.,* 1998; Zaborski 1998, 2000)

According to Ayok *et al*. (2013), the Kanawa Formation in the Gulani area comprises shales with phosphatic condensed horizon in its lower part and a number of thin bioclastic limestones in its upper part, representing, respectively, the deeper and shallower-water portions of the "Kanawa Formation Sea". Its littoral facies would be expected to have occurred somewhere towards the east and to have become subaerially exposed during the mid-Turonian regression and progressively eroded and redeposited to the west. The Gulani Formation, therefore, may be, in large part, composed of reworked Late Cenomanian to Early Turonian sands (see Fig.8). Sedimentary sources within the older Yolde Formation and upper part of the Bima Group are possible, but less likely as they generally contain finer-grained sandstones than those characterizing the Gulani Formation.

CONCLUSION

Palaeocurrent directions for the Gulani Formation show a westerly-directed radiating pattern, suggesting the main point of sediment influx was located around latitude 10^{o}46' north.

Petrographically, the cross-bedded sandstones subfacies is medium to very coarse-grained, poorly to well sorted, sub-angular to well rounded quartz arenite consisting of majorly monocrystalline quartz and rare polycrystalline quartz with a kaolinitic matrix.

The extreme rarity or absence of feldspar in the sandstones of the Gulani Formation and the lack of discernable evidence of its digenetic lost (either dissolution or decomposition), the presence of sedimentary rock fragments and the low-diversity heavy mineral assemblage suggests a sedimentary source, perhaps reworked Late Cenomanian to Early Turonian littoral sands deposited during a preceding transgressive interval.

ACKNOWLEDGEMENTS

This work was an offshoot of a broader and more detailed account on the study of the Gulani Formation carried out at the Department of Geology, Ahmadu Bello University, Zaria under the tutelage of Prof. P.M. Zaborski as part of the author's PhD dissertation. This work was partly funded by the Ahmadu Bello University, Zaria Board of Research Grant and Carnegie Foundation Grant (ie Dissertation Completion Grant). I also want to sincerely acknowledge the Polish UNESCO for awarding six months fellowship to me and the host Institution, Department of Fundamental Geology, Faculty of Science, University of Silesia, Poland.

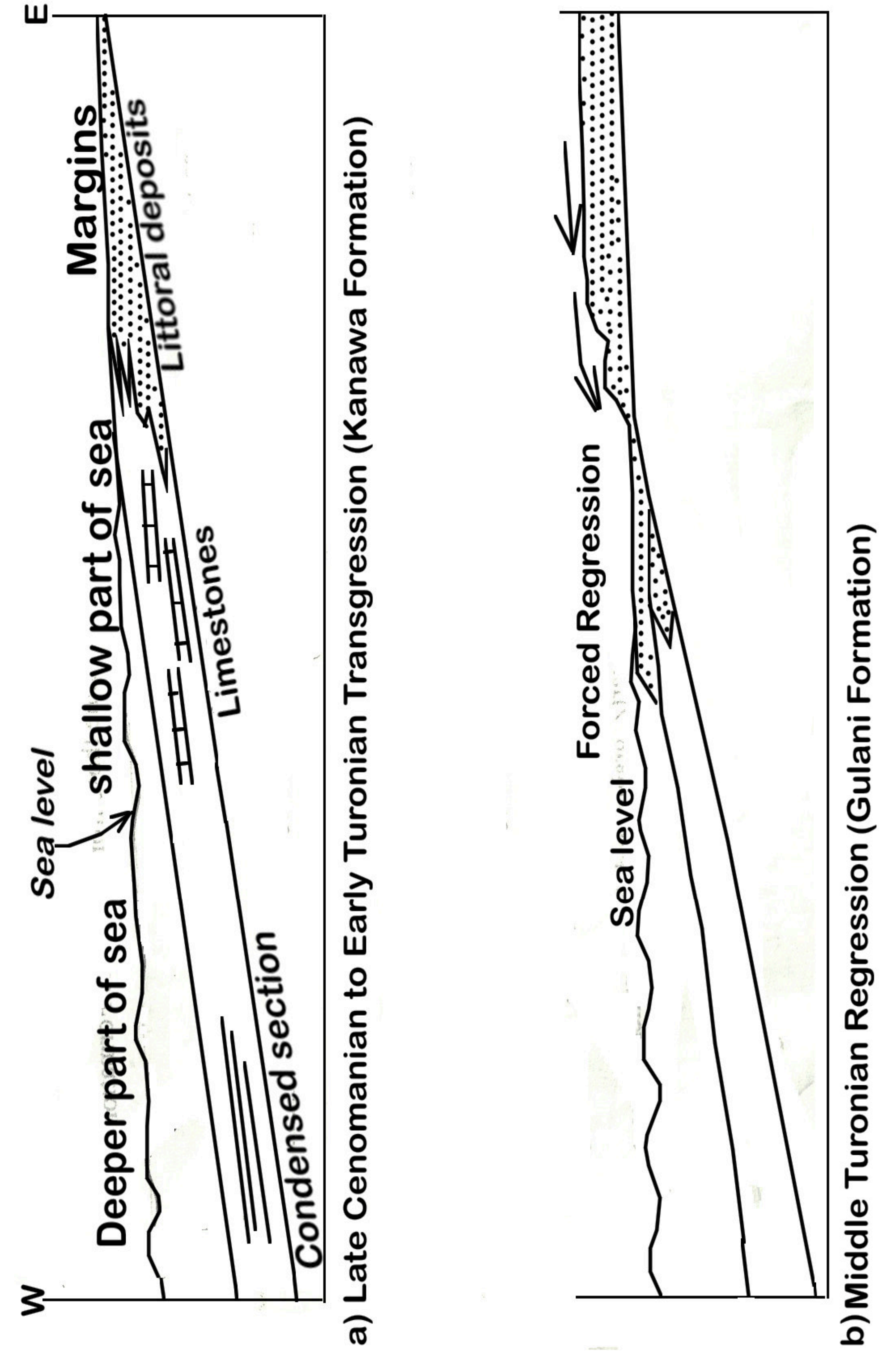

Fig. 8: Model showing the proposed depositional environments in the eastern Gongola Basin during the Late Cenomanian to Early Turonian transgression and subsequent Middle Turonian regression

REFERENCES

Ayok, J. Zaborski, P. M. and Hamza. H. (2013). A sequence stratigraphic interpretation of the Late Cretaceous Kanawa and Gulani formations in the eastern Gongola Basin of the Benue Trough, North-East Nigeria. *African Geoscience Review*, 20, 1-12.

Ayok, J. Zaborski, P. M. Danbatta U.A. and Hamza. H. (2014). The Gulani Formation (Turonian) in the eastern Gongola Basin, north-east Nigeria: a re-evaluation of the lithostratigraphic status. *Journal of Mining and Geology*, 50 (1), 41-51.

Ayok, J. and Zaborski, P. M. (2014). Facies analysis within the Turonian Gulani Formation, eastern Gongola Basin, northeastern Nigeria. *African Geoscience Review*, 21, 79-87.

Basu, A., 2003. A perspective on quantitative provenance analysis. In: Valloni, R., Basu, A. (Eds.), Quantitative Provenance Studies in Italy, *Memorie Descrittive della Carta Geologicadell'Italia*, 61: 11 – 22.

Busson, G. (1972). Principes, méthods et résultants d'une étude stratigraphique du Mésozoïque saharien. *Mémoir Museum National a'Histoire naturelle* (Paris) (n.s.), 26, 1-441.

Carter, J. D; Barber, W; Tait, E. A. and Jones, G. P. (1963). The geology of Parts of Adamawa, Bauchi and Borno Provinces in North-eastern Nigeria. *Bulletin of the Geological Survey of Nigeria*, 30, 1 – 108.

Cuthbert, S.J., (1991). Evolution of the Devonian Hornelen basin, west Norway: new constraints from petrological studies of metamorphic clasts. In: Morton, A.C., Todd, S.P., Haughton, P.D.W. (Eds.), Developments in Sedimentary Provenance Studies. Geological Society of London Special Publication. 57: 343– 360.

Fairhead, J. D. (1986). Geophysical controls on sedimentation within the African rift systems. *Special Publication Geological Society of London*, 25, 19-27.

Guiraud, M. (1990). Tectono-sedimentary framework of the Early Cretaceous continental Bima Formation (Upper Benue Trough, (NE) Nigeria). *Journal of African Earth Science*, 10, 341 – 353.

Hamidu, I. Zaborski, P. M. and Hamza. H. (2013). A review of the Campanian to Maastrichtian lithostratigraphic succession in the Cretaceous Gongola Basin of north-east Nigeria. *Journal of Mining and Geology*, 49 (2),145-160.

Meister, C., Alzouma, K., Lang, J. and Mathey, B. (1992). Les ammonites du Niger (Afrique occidentale) et la transgression transsaharienne au cours du Cénomanian-Turonien. *Geobios*, 25, 55-100.

Pettijohn, F. J., Potter, P. E. & Siever, R. (1987). *Sand and Sandstone*, (*2nd edition*). Springer, New York. 553 pp.

Popoff, M, Wiedmann, J. and Wasz, I. (1986). The Upper Cretaceous Gongila and Pindiga Formations, Northern Nigeria. Subdivisions, age, stratigraphic correlations and paleogeographic implications. *Eclogae Geologicae Helvetiae*, 79, 343 – 363.

Reyment, R. A. (1980). Biogeography of the Saharan Cretaceous and Paleocene epicontinental transgressions. *Cretaceous Research*, 1, 299-327.

Weltje G. J. & von Eynatten H. (2004). Quantitative provenance analysis of sediments: a review and outlook. *Sedimentary Geology*, 171: 1 – 11.

Zaborski, P. M. (1998). A review of the Cretaceous System in Nigeria. *Africa Geoscience Review*, 5, 385 – 483.

Zaborski, P. M. (2000). The Cretaceous and Paleocene trangressions in Nigeria and Niger. *Journal of Mining and Geology*, 36, 153-173.

Zaborski, P. M. (2003). Guide to the Cretaceous System in the Upper Part of the Upper Benue Trough, North-Eastern Nigeria. *Africa Geoscience Review*, 10, 13 – 32.

Zaborski, P. M., Ugodulunwa, F., Idornigie, A., Nnabo, P. and Ibe, K. (1998). Stratigraphy and Structure of the Cretaceous Gongola Basin, northeast Nigeria. *Bulletin de Centres des Recherches Exploration Production Elf-Aquitaine*, 21, 153 – 186.

APPENDIX A.1

Maliya Section (Eastern limb of Jana Syncline)

Foreset Dip (field Reading)	Tectonic Dip	Corrected foreset dip
08°@288°	11°@145°	18°@307°
20 °@292°	"	29°@303°
18 °@310 °	"	28 °@315°
28 °@318 °	"	39 °@320°
22 °@290 °	"	32 °@292°
30 °@320 °	"	41 °@322°
18 °@312 °	"	29 °@319°
18 °@308 °	"	28 °@314°
34 °@260 °	"	39 °@276°
18 °@300 °	"	28 °@311°
20 °@270 °	"	29 °@292°
18 °@270 °	"	26 °@292°
20 °@250 °	"	32 °@290°
28 °@268 °	"	44 °@296°
22 °@270 °	"	30 °@292°
20 °@264 °	"	28 °@286°
12 °@270 °	"	20 °@294°
26 °@274 °	"	34 °@292°
26 °@268 °	"	33 °@284°
32 °@290 °	"	42 °@301°
10°@196°	"	04°@246°
40°@234°	"	41°@249°
19$_o$@228°	"	20@202°
18°@228°	"	20@204°
20°@232°	"	21@206°

APPENDIX A.2

Gulani Section

Foreset Dip (field Reading)	Tectonic Dip	Corrected foreset dip
29°@230°	11 °@164 °	27°@252°
22@232 °	"	23°@262°
36@240 °	"	36°@259°
47@221 °	"	43°@237°
41@220 °	"	30°@235°
36°@216°	"	32°@234°
40@217°	"	36°@233°
39@274°	"	44°@291°
43@204°	"	38°@222°
37@238°	"	36°@257°
36@214°	"	30°@230°
31@264°	"	36°@287°
27@248°	"	29°@273°
31@221°	"	18°@252°
35@237°	"	34°@255°
34@236°	"	34°@257°
37@216°	"	33°@232°
35@242°	"	34°@262°
33@224°	"	31°@246°
37@242°	"	36°@262°

APPENDIX A.3

Tashan Garba Section (Western trusted limb of Jana Syncline)

Foreset Dip (Field Reading)	Tectonic Dip	Corrected foreset dip
08º@162º	36º@128º	29º@298º
18º@162º	"	24º@280º
14º@162º	"	26º@290º
18º@162º	"	24º@280º
10º@162º	"	28º@296º
14º@162º	"	26º@290º
20º@162º	"	24º@276º
17º@160º	"	24º@284º
20º@160º	"	23º@276º
30º@160º	"	29º@253º
14º@160º	"	27º@289º
12º@160º	"	26º@294º
18º@160º	"	24º@284º
18º@160º	"	24º@284º
22º@160º	"	23º@272º
20º@160º	"	23º@276º
22º@160º	"	23º@272º
08º@168º	"	30º@296º
16º@168º	"	26º@284º
02º@168º	"	34º@303º
04º@168º	"	32º@300º
18º@164º	"	25º@281º
14º@168º	"	28º@287º
12º@168º	"	29º@290º
12º@162º	"	28º@292º
15º@156º	"	25º@289º
08º@170º	"	30º@296º
18º@164º	"	25º@281º
22º@162º	"	23º@274º
22º@160º	"	23º@272º

APPENDIX A.4

Eastern limb of Balbaya Syncline

Foreset Dip (Field Reading)	Tectonic Dip	Corrected foreset dip
40º@192º	18º@114º	39º@220º
40º@220º	"	39º@248º
40º@202º	"	39º@232º
50º@230º	"	46º@254º
18º@198º	"	17º@252º
44º@220º	"	42º@245º
42º@182º	"	39º@214º
33º@212º	"	31º@246º
32º@202º	"	31º@236º
38º@220º	"	37º@250º
50º@240º	"	43º@260º
40º@196º	"	39º@227º
40º@210º	"	39º@238º
40º@210º	"	39º@238º
30º@200º	"	29º@236º
30º@214º	"	29º@250º
40º@220º	"	39º@250º
30º@196º	"	29º@237º
40º@200º	"	39º@230º

APPENDIX B.1

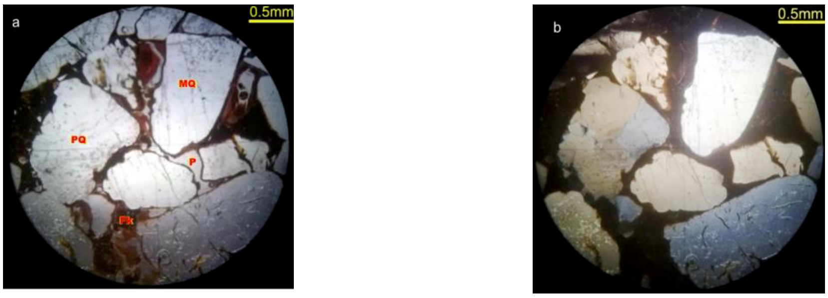

Figure 9. Photomicrograph of Gulani Formation, type section, north-east of Dogon Zaga, showing sandstone from unit DZ25 of Fig. 3 (P-pore space; PQ-polycrystalline quartz; MQ-monocrystalline quartz; Fk-ferruginized kaolinite (note, section >30µm). a) PPL b) XPL.

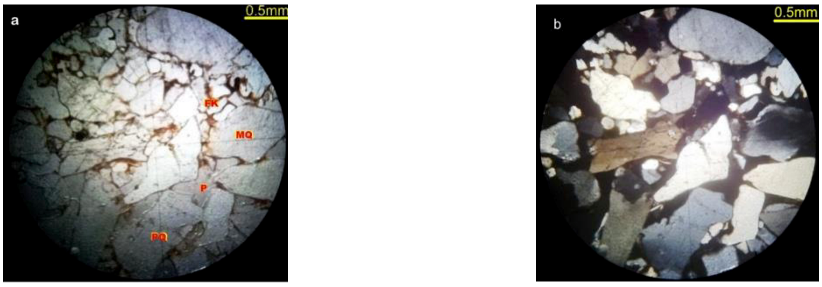

Figure 10. Photomicrograph of Gulani Formation, type section, north-east of Dogon Zaga, showing sandstone from unit DZ21 of Fig. 3; (P-pore space; PQ-polycrystalline quartz; MQ- monocrystalline quartz; Fk-ferruginized kaolinite; (note, section >30µm in thickness). a) PPL and b) XPL.

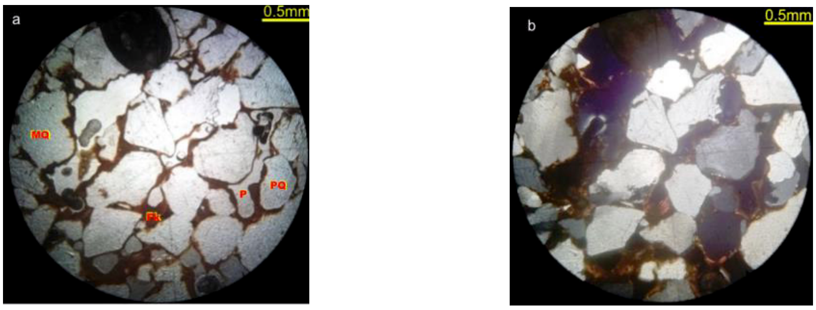

Figure 11. Photomicrograph of Gulani Formation, type section, north-east of Dogon Zaga, showing sandstone from unit DZ17 of Fig. 3; (P-pore space; PQ-polycrystalline quartz; MQ-monocrystalline quartz; Fk-ferruginized kaolinite). a) PPL and b) XPL.

APPENDIX B.1

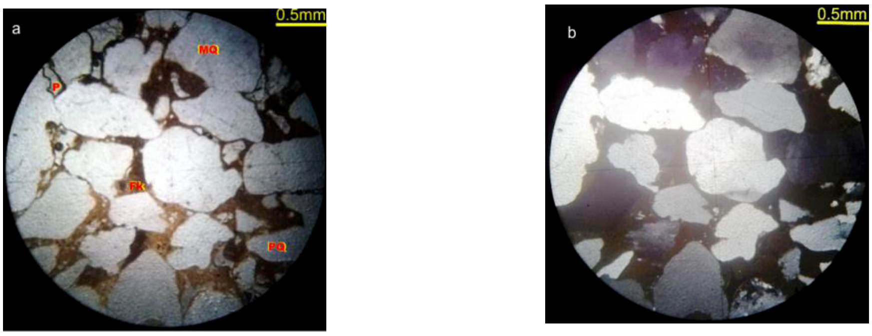

Figure 12. Photomicrograph of Gulani Formation, 750 m north of Gulani, showing sandstone from unit G13 of Fig. 4 (P-pore space; PQ-polycrystalline quartz; MQ-monocrystalline quartz; Fk-ferruginized kaolinite). a) PPL and b) XPL.

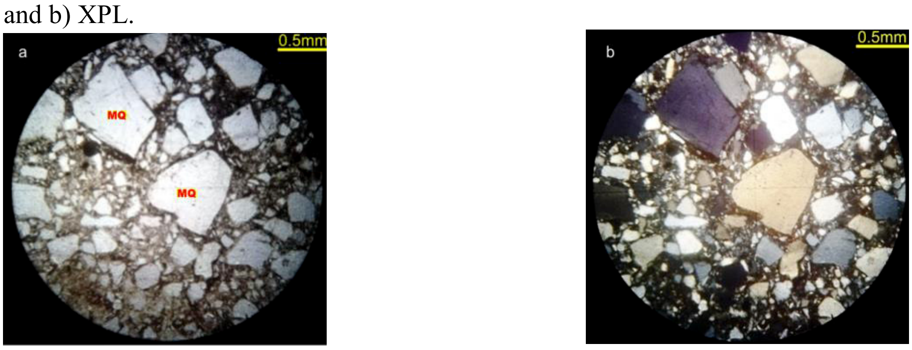

Figure 13. Photomicrograph of Gulani Formation, 750 m north of Gulani, showing sandstone from unit G11 of Fig. 4 (MQ-monocrystalline quartz). a) PPL and b) XPL. (note: section thickness >30µm).

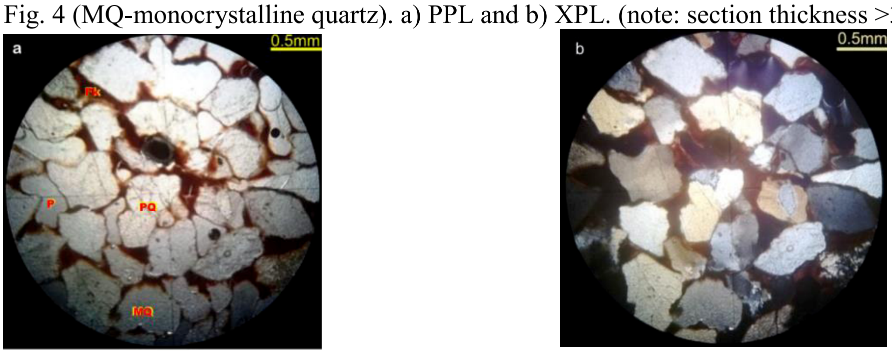

Figure 14. Photomicrograph of Gulani Formation, 750 m north of Gulani. showing sandstone from unit G09 of Fig. 4 (P-pore space; PQ-polycrystalline quartz; MQ-monocrystalline quartz; Fk-ferruginized kaolinite). a) PPL and b) XPL. (note: section thickness >30µm).

APPENDIX B.3

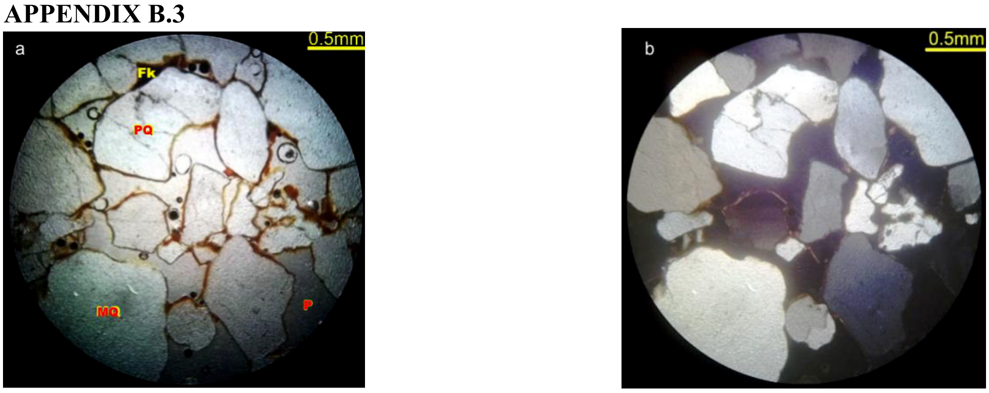

Figure 15. Photomicrograph of Gulani Formation, 100 m west of Maliya, showing sandstone from unit M21 of Fig. 5 (P-pore space; PQ-polycrystalline quartz; MQ-monocrystalline quartz; Fk-ferruginized kaolinite). a) PPL and b) XPL.

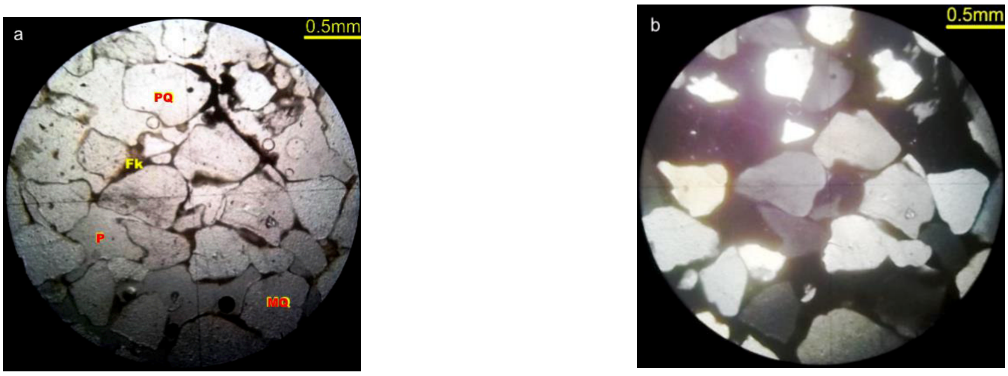

Figure 16. Photomicrograph of Gulani Formation, 100 m west of Maliya, showing sandstone from unit M19 of Fig. 5 (P-pore space; PQ-polycrystalline quartz; MQ-monocrystalline quartz; Fk-ferruginized kaolinite). a) PPL and b) XPL.

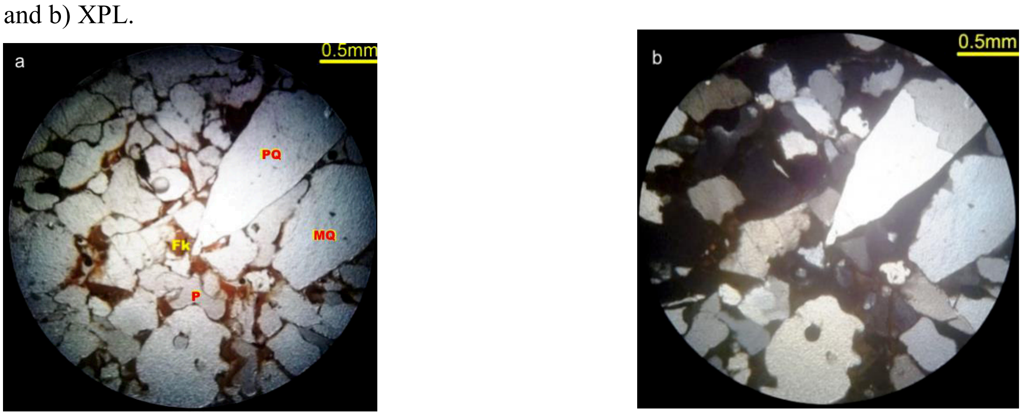

Figure 17. Photomicrograph of Gulani Formation, 100 m west of Maliya, showing sandstone from unit M01 of Fig. 5 (P-pore space; PQ-polycrystalline quartz; MQ-monocrystalline quartz; Fk-ferruginized kaolinite). a) PPL and b) XPL.